Journal of Atmospheric and Terrestrial Physics, Vol. 49, No. 3, pp. 217–229, 1987.
Printed in Great Britain.

0021–9169/87 $3.00 + .00
Pergamon Journals Ltd.

Time domain polarization analysis of Schumann resonance waveforms

A. TZANIS* and D. BEAMISH

British Geological Survey, Murchison House, West Mains Road, Edinburgh EH9 3LA, U.K.

(*Received in final form* 22 *April* 1986)

Abstract—Schumann resonance waveforms in the lower ELF band are produced by distant lightning discharges. The multiplicity of world-wide thunderstorm centres provides a background spectrum which is generally incoherent. Superimposed on this background are larger amplitude events from individual thunderstorm centres. Source direction finding requires the determination of the polarization properties of these complex and superimposed waveforms. A time domain polarization analysis technique is described and applied to a variety of examples of Schumann resonance waveforms. The background waveforms display the anticipated level of incoherent polarization properties. It is demonstrated that the technique can isolate individual waveforms that are linearly polarized and which represent the arrival of short path signals from single source locations.

INTRODUCTION

In the ELF band (5 Hz–25 kHz) electromagnetic energy is largely produced as radiation from vertical lightning discharges. It is estimated that of the order of 100 lightning flashes occur each second (TURMAN and EDGAR, 1982). Such sources may contain a wide spectrum of frequencies, however, for distant sources the energy undergoes multiple reflection in the Earth–ionosphere cavity giving rise to frequency dependent attenuation. The main energy components in the lower ELF band (5 Hz–2 kHz) are the Schumann resonance modes. The energy propagates as a transverse magnetic mode in which the electric field is largely radial and the magnetic field horizontal (MADDEN and THOMSON, 1965). Although the polarization characteristics of the horizontal magnetic field are required to successfully locate a discharge centre (KEMP, 1971; BLIOKH *et al.*, 1980), only a few examples of the polarization properties of ELF waveforms have appeared in the literature.

The data used in the present analysis have been previously examined in the high-resolution spectral study of BEAMISH and TZANIS (1986). The AudioMagnetoTelluric (AMT) instrumental conditioning and collection scheme provides four decades of data from 100 to 0.01 Hz. Decade 1 data are sampled at 200 Hz and provide a data bandwidth from 100 to 10 Hz. This decade attenuates the fundamental (7.5 Hz) Schumann resonance mode but provides data for studies of the higher order modes. It is data from this decade, part of the lower ELF band, that is the subject of the present study. The data were collected in western Anatolia (Turkey); geographic coordinates 40.5°N, 30.0°E.

In general, Schumann resonance waveforms comprise 'events' superimposed on a background. The spectral content of typical decade 1 data has been described by BEAMISH and TZANIS (1986). Stable Schumann resonance modes are consistently resolved at 14.0, 21.0, 27.0, 33.5 and 39.5 Hz by integrating the spectrum over real time windows of approximately 90 s. An examination of the time local spectral properties of Schumann waveforms revealed large variability in power spectral densities and their frequency content. The sonogram of Fig. 1 is used to illustrate this behaviour. The lowest power levels arise from the continuum of background activity. The peak power levels are due to large amplitude transient events. JONES and KEMP (1970, 1971) indicate that for a given ionosphere the spectral structure of Schumann waveforms is strongly dependent on distance from the source. BEAMISH and TZANIS (1986) attributed the spectral variability indicated in Fig. 1 to the effect of signals being received from a variety of distributed source locations. The present polarization analysis of the horizontal magnetic field enables this assertion to be examined in detail.

In order to extract realistic polarization parameters for the waveforms considered it has been necessary to investigate suitable time local polarization techniques.

*Also at: Geophysics Department, University of Edinburgh, Kings Buildings, J.C.M.B., Mayfield Road, Edinburgh, U.K.

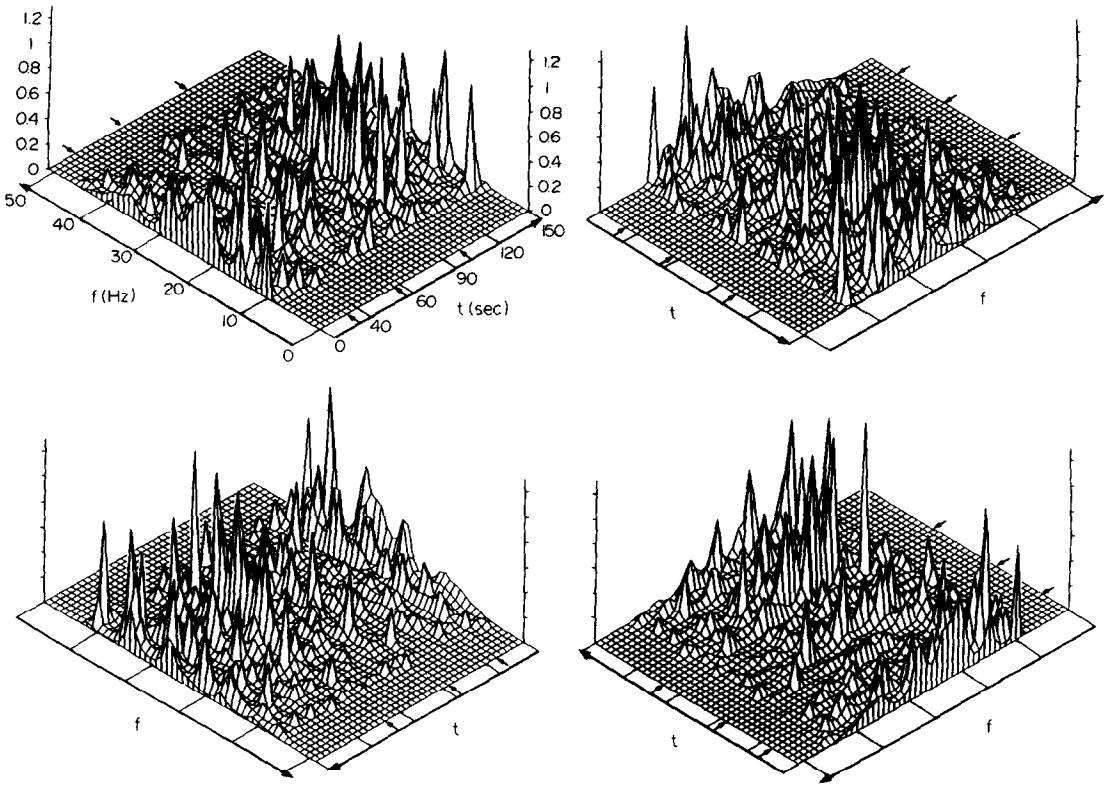

Fig. 1. High resolution sonogram of the N–S (H) magnetic component. Four perspective views of the same sonogram. Data collected on 8 June 1984. Power density values in $(nT)^2\ Hz^{-1} \times 10^{-6}$; $n = 2, 3, 4, 5, 6$ modes; decade 1 data; Maximum Entropy power spectra (see BEAMISH and TZANIS, 1986); filter length $M = 35$.

A monochromatic, elliptically-polarized wave of angular frequency w may be defined by its two orthogonal components

$$x(t) = X(t) \cdot \cos\left[wt + \phi_x(t)\right],$$

$$y(t) = Y(t) \cdot \cos\left[wt + \phi_y(t)\right],$$

e.g. the two horizontal magnetic components (H, D). The basic theory of polarization analysis is then as given by BORN and WOLF (1959) and repeated by FOWLER *et al.* (1967). The polarization characteristics are usually derived by examining the coherence or cross-spectral matrix between the two components. Such characteristics are obtained in the *frequency* domain across appropriate time averages. In the present study we adopt a technique which permits the derivation of polarization parameters in the time domain, in the form of instantaneous values. The advantage of this approach is that it permits the tracing of any variation in the state of *individual* waveforms encountered within a particular data window.

DATA ANALYSIS AND THE CONCEPT OF A COMPLEX SIGNAL

KODERA *et al.* (1977) describe a method for the analysis of polarization of any two orthogonal components (x, y) based on the complex representation of a polarized signal. The technique was first described by GABOR (1946). The technique extends the formalism obeyed by an *analytic* signal to a two component representation. The method proposed by KODERA *et al.* (1977) was primarily intended for measurements made in rotating frames of reference (satellites and spacecraft), but it is also suitable for a wide range of applications, such as narrow band or linearly polarized signals in fixed, although arbitrary, frames of reference. Our AMT data exhibit large waveform variability and are recorded in relatively narrow band schemes over time intervals comparable to those of many transient ELF events. In the present study we use the same mathematical formulation as KODERA *et al.* (1977), but a different numerical implementation. A detailed account of the formalism

can be found in KODERA *et al.* (1977) and only a brief description is provided here.

For a given monochromatic signal $x(t)$, defined by

$$x(t) = X(t) \cdot \cos [wt + \phi(t)],$$

a complex or analytical signal $x_a(t)$ may be defined by

$$x_a(t) = x(t) + i\bar{x}(t),$$

where $\bar{x}(t)$ is the Hilbert transform of $x(t)$. The instantaneous amplitude $X(t)$, the instantaneous phase $\phi(t)$ and the instantaneous frequency $f(t)$ are then given by

$$X(t) = [x^2(t) + \bar{x}^2(t)]^{1/2},$$

$$\phi(t) = \tan^{-1} [\bar{x}(t)/x(t)],$$

$$f(t) = \frac{d}{dt} [\phi(t)].$$

The complex signal associated with a real signal having two orthogonal components (x, y) is simply defined as

$$c(t) = x(t) + iy(t).$$

KODERA *et al.* (1977) demonstrate that it is possible to express the complex signal in terms of circular components rotating in opposite directions. At any given frequency w_0 we may write

$$c(t, w_0) = C(w_0) \cdot \exp (iw_0 t),$$

which represents a circular harmonic in the complex plane rotating in a sense depending on the sign of w_0. Positive frequencies correspond to polarized signals rotating in the positive (counterclockwise) sense and negative frequencies to signals rotating in the negative (clockwise) sense. The power spectrum of the complex signal is related to the intensity of the circular components and the spectral asymmetry is linked to the polarization of the real signal.

It is possible to divide the frequency spectrum of the complex signal into two parts, corresponding to positive (+) and negative (−) frequencies, such that

$$C(w) = C+(w) + C-(w).$$

By inverse Fourier transformation we then obtain

$$c(t) = c+(t) + c-(t).$$

KODERA *et al.* (1977) show how these circular decomposites of the complex signal can be expressed in terms of the analytic signals for x and y. The expressions are

$$c+(t) = [x_a(t) + iy_a(t)]/2,$$

$$c-(t) = [x_a^*(t) + iy_a^*(t)]/2.$$

The polarization parameters are conventionally expressed in terms of the amplitudes and phases of the two orthogonal components. The above formulation, however, provides expressions in terms of the circular components of the signal. A circular signal is not affected by the orientation of the coordinate system and therefore the amplitude of the complex signal remains invariant and all the information about the polarization axis is contained in the phase term. We now go on to obtain the relationships between the conventional polarization parameters and the two circular components $c+$ and $c-$. We consider the case of monochromatic, elliptically-polarized signals only.

Consider two circular components as given above with

$$c+(t) = A_1 \cdot \exp [i(wt + \phi_1)],$$

$$c-(t) = A_2 \cdot \exp [i(wt + \phi_2)].$$

When the two components are in phase the signal reaches the maximum amplitude ($|A_1 + A_2|$), which represents the major axis of the polarization ellipse. When they are out of phase the signal reaches its minimum amplitude ($|A_1 - A_2|$), which represents the minor axis of the polarization ellipse. The polarization parameters are therefore simply obtained as

$$\text{half major axis: } a = |c+| + |c-|,$$

$$\text{half minor axis: } b = |c+| - |c-|,$$

$$\text{ellipticity: } E = b/a,$$

$$\text{azimuth: } \theta = [\arg(c+) + \arg(c-)]/2.$$

In these expressions b and E are positive for counterclockwise rotation, and vice versa. Although all the above expressions assume monochromatic waveforms, KODERA *et al.* (1977) suggest that these formulae may also be used to obtain instantaneous polarization parameters for non-monochromatic real signals. The numerical implementation of the procedure is described in detail by TZANIS and BEAMISH (1986).

TIME DOMAIN HODOGRAMS

Prior to the presentation of the polarization properties obtained using the above procedures, we first examine simple time domain hodograms. Throughout the results presentation we use 150 data points of decade 1 data with a sampling rate of 200 Hz. The components used are the two horizontal magnetic field components (H, D), expressed in nT. Time domain hodograms simply plot the locus of the rotation vector of the two orthogonal components in

the horizontal plane. For a given data window (150 points) we may plot the rotation vector over the whole window or over selected subsets. Here we display the two components over the whole data window and plot hodograms for the five successive subsets of 30 points encountered within each window. The hodograms of each subset are independently scaled. The procedure thus approximates the selection of individual waveforms.

The data were collected at a single site on 26 July 1984 commencing at 12.40 h (local time). The results from three data windows are shown in Fig. 2. The largest peak-to-peak amplitudes are all less than 0.05 nT, and where waveform amplitudes fall below 0.01 nT we begin to encounter noise. The RUN numbers refer to the collection number of each data window. Successive data windows are separated by approximately 3 s in real time. We present the results to convey the general complex nature of the sferic waveforms encountered. It can be seen that the waveforms provide the whole range of elliptical polarization properties from linear through to quasi-circular. It can also be seen that the time domain hodograms offer only a relatively crude method of presenting the polarization characteristics of these complex waveforms.

TIME DOMAIN POLARIZATION OF BACKGROUND SFERICS

Detailed polarization results are now presented for 3 data windows which we consider to be representative of background sferic source fields. The data were collected at a single site on 8 June 1984 commencing at 10.40 h (local time). The same method of presentation is repeated for all three examples. For each example shown in Fig. 3 the polarization parameters ellipticity (E) and azimuth (θ) are plotted in the time domain below the corresponding data. This method of display enables the variations in the state of polarization of individual waveforms to be monitored. The results obtained have been fully verified using the above simpler techniques. The instantaneous values of (E, θ) consist of a series of discrete symbols that correspond to the extrema in (H, D), i.e. the signal inflexion points evaluated using the modulus. If the modulus falls below 20% of the maximum excursion encountered the result is omitted. This method of display is a simple and effective method of suppressing the contributions from low amplitude waveforms. In keeping with the previous definitions, a value of $E = 1$ corresponds to a circular wave rotating counterclockwise, a value of $E = 0$ corresponds to a linearly polarized wave and a value of $E = -1$ to a circular wave rotating in a

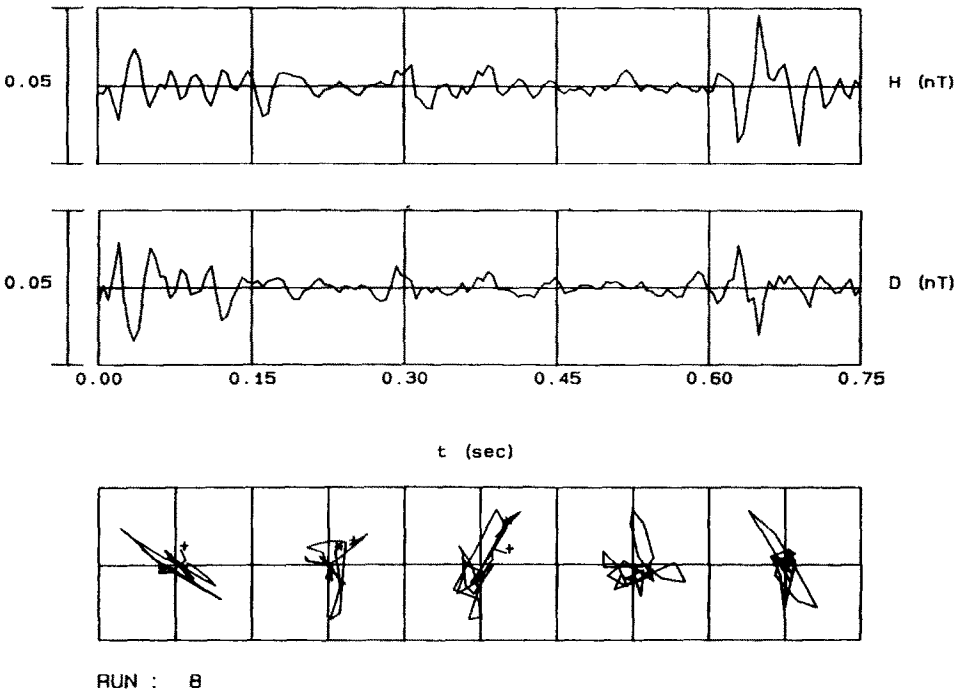

Fig. 2. Time domain hodograms. H and D correspond to the magnetic N–S and E–W components.
(*Continued over.*)

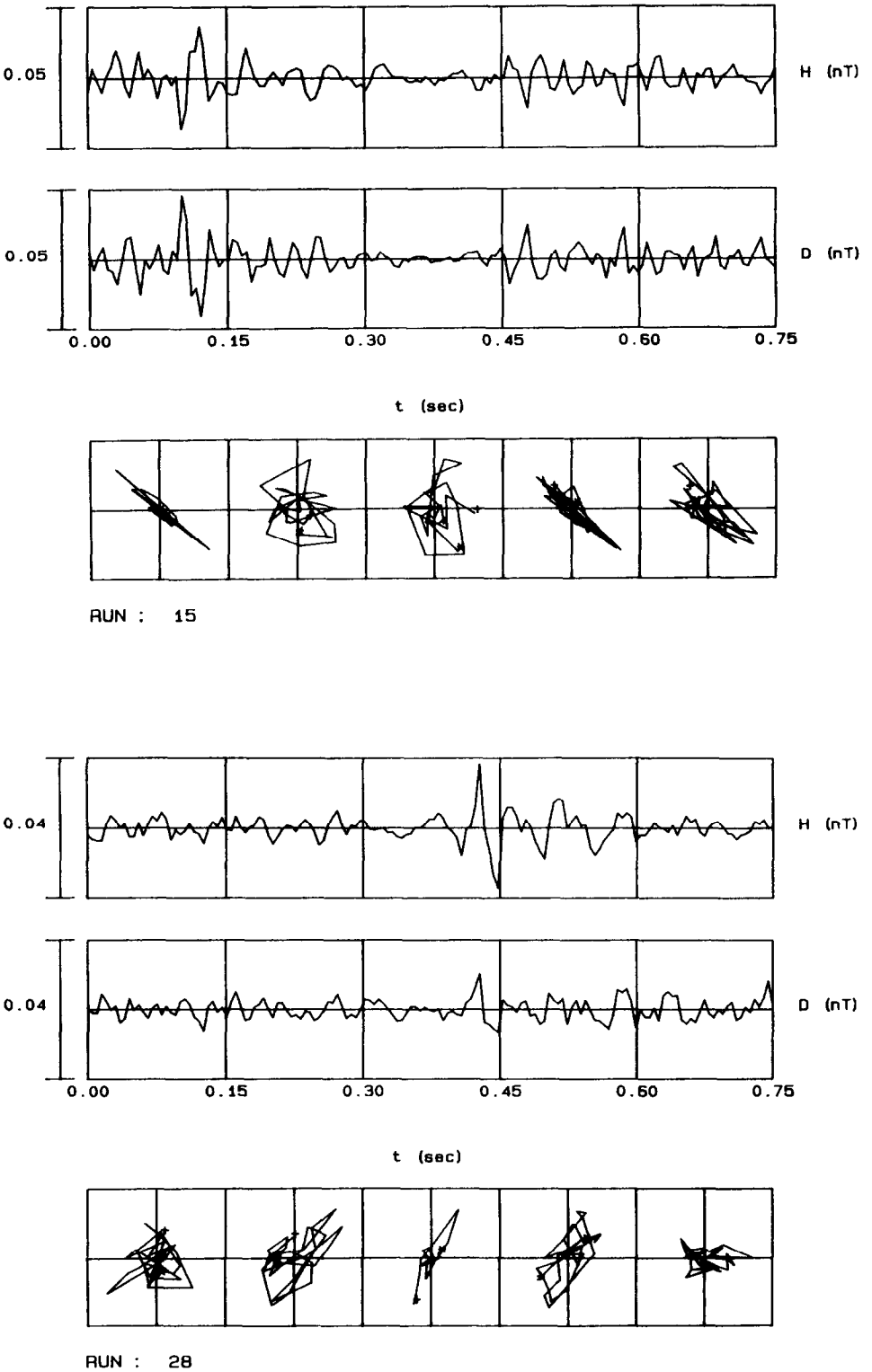

Fig. 2 continued.

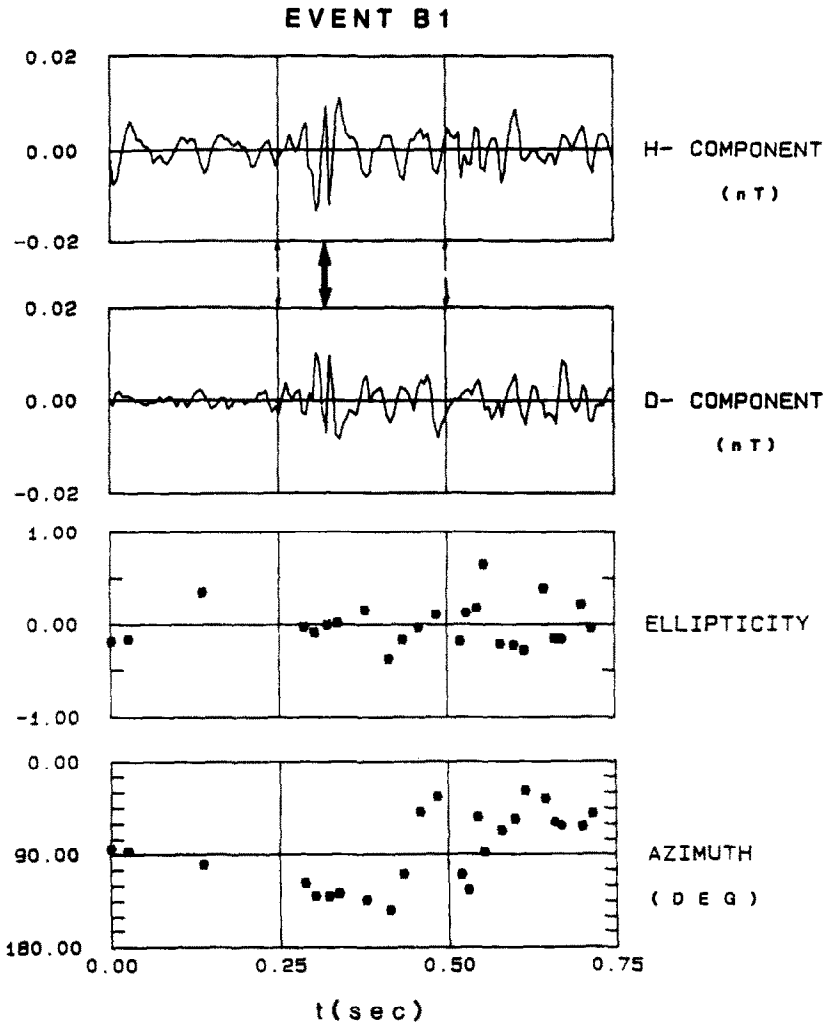

Fig. 3. Three examples of the time domain polarization analysis of background sferics. *H* and *D* correspond to the N–S and E–W magnetic components; real time separation of events B1–B2, 37.5 s, events B2–B3, 45.00 s. (*Continued over.*)

clockwise sense. Azimuths are defined in magnetic coordinates of west (180°), north (90°) and east (0°).

It can be seen from the examples provided in Fig. 3 that the largest peak-to-peak amplitude is of the order of 0.03 nT. The peak-to-peak amplitude of the general background appears to be less than 0.01 nT for this particular day. The full range of ellipticities and azimuths appear to be sampled, although none of the waveforms could be considered to be circularly polarized. According to BLIOKH *et al.* (1980), the background waveforms are the response of the cavity to the nearly continuous global sum of lightning activity. The waveforms received are thus the superposition of arrivals from multiple and incoherent sources. If this is the case, the polarization characteristics of background waveforms should be effectively random. Such characteristics are observed most acutely in many of the waveforms of Fig. 3b.

When we consider several of the larger amplitude events shown in Fig. 3 (indicated by thick arrows) we note a tendency for the waveforms to be linearly polarized at a given azimuth. The azimuths are different in each case and the polarization characteristics remain stable over several cycles. It therefore appears that the present method of analysis is capable of detecting 'background level' resonance waveforms from individual source locations. The data windows shown above belong to the same ensemble that was used to construct the sonogram of Fig. 1, and their approximate position is indicated with arrows.

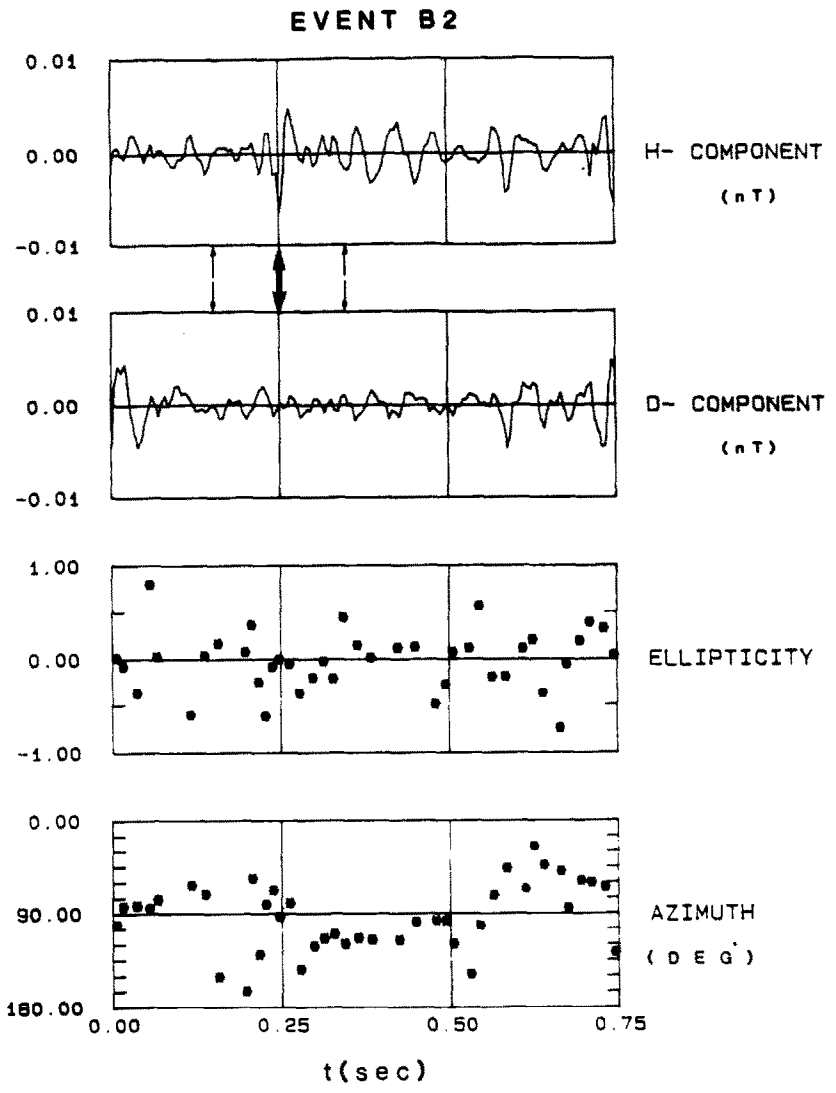

Fig. 3 continued. (*Continued over.*)

TIME DOMAIN POLARIZATION OF IMPULSIVE SFERICS

Detailed polarization results are now presented for three data windows which we consider to be representative of larger amplitude, impulsive ELF fields. According to JONES and KEMP (1971), such events are due to the transient excitation of the cavity resonance by unusually large lightning discharges. The data were collected at a single site on 27 July 1986 commencing at 10.37 h (local time). The three examples of impulsive events shown in Fig. 4 all have peak-to-peak amplitudes greater than 0.03 nT, the largest being of the order of 0.1 nT (Fig. 4b). The impulsive waveforms can all be characterized as damped, quasi-sinusoids. The three examples all possess the characteristic commencement of typical transient events noted by JONES and KEMP (1971). The initial part of each waveform is due to the arrival of the direct (short path) signal. Subsequent fluctuations are due to the arrival of the long path signal and to the circulation of the energy around the globe. It is quite evident from the polarization results that these waveforms are linearly polarized at a particular azimuth and the azimuths differ for each of the three examples. The two main waveforms encountered in Fig. 4b provide a good example of single source repetition on a time scale of 0.5 s.

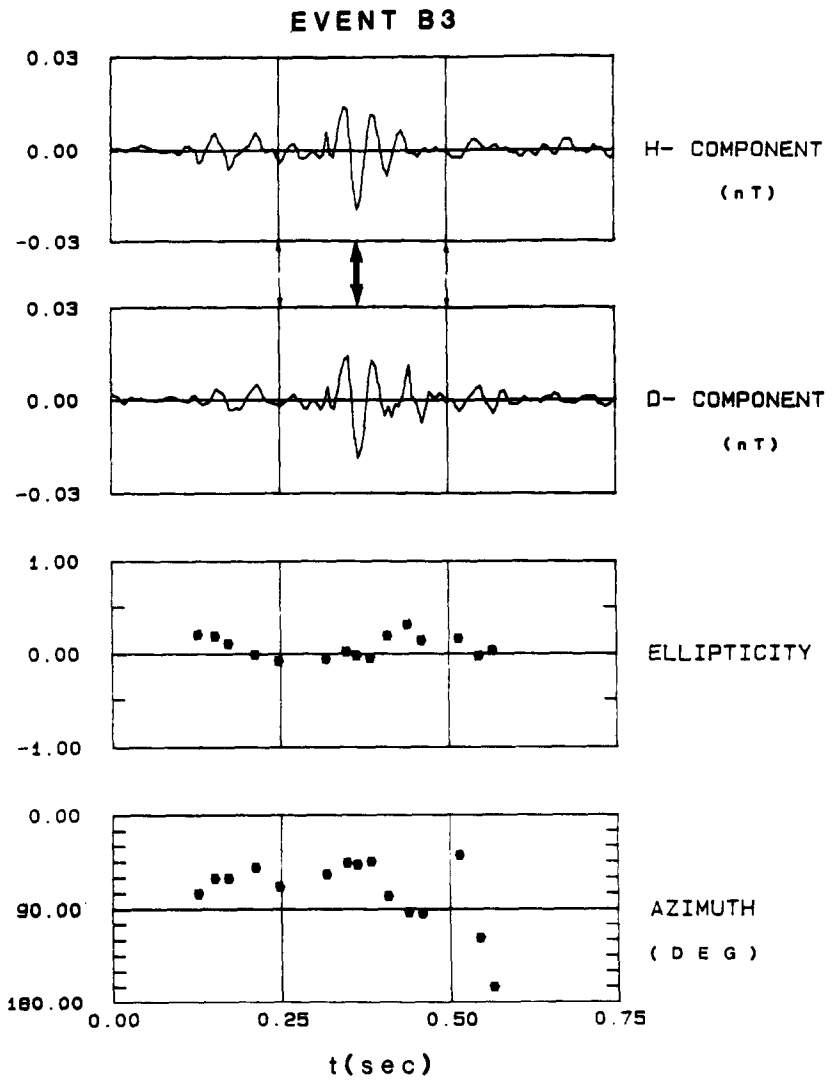

Fig. 3 continued.

SPECTRAL SIGNATURES OF THE EXAMPLE SFERICS

The polarization analysis of the background and impulsive Schumann resonance waveforms reveals that they contain a variety of events with a wide range of polarization vectors, which indicates the existence of distributed sources and simultaneous thunderstorm activity.

The theoretical and experimental work of JONES and KEMP (1970, 1971) and KEMP (1971) suggests that the spectral shape, i.e. the relative position of peaks and troughs, is a function of the source receiver separation for a specified ionosphere. Given the azimuthal distribution of the sources, it is anticipated that the spectral signature of our example waveforms will vary in a manner characteristic of the source spectrum and the propagation distance. This could account for the extremely variable time local behaviour of the Schumann resonances, as indicated in Fig. 1 (see also fig. 9 of BEAMISH and TZANIS, 1986). We now proceed to investigate this assertion.

In Fig. 5a–c we present the power spectra for the azimuthal (total horizontal) magnetic field of the example background events, annotated B1, B2 and B3, respectively, and in Fig. 5d–f the equivalent power

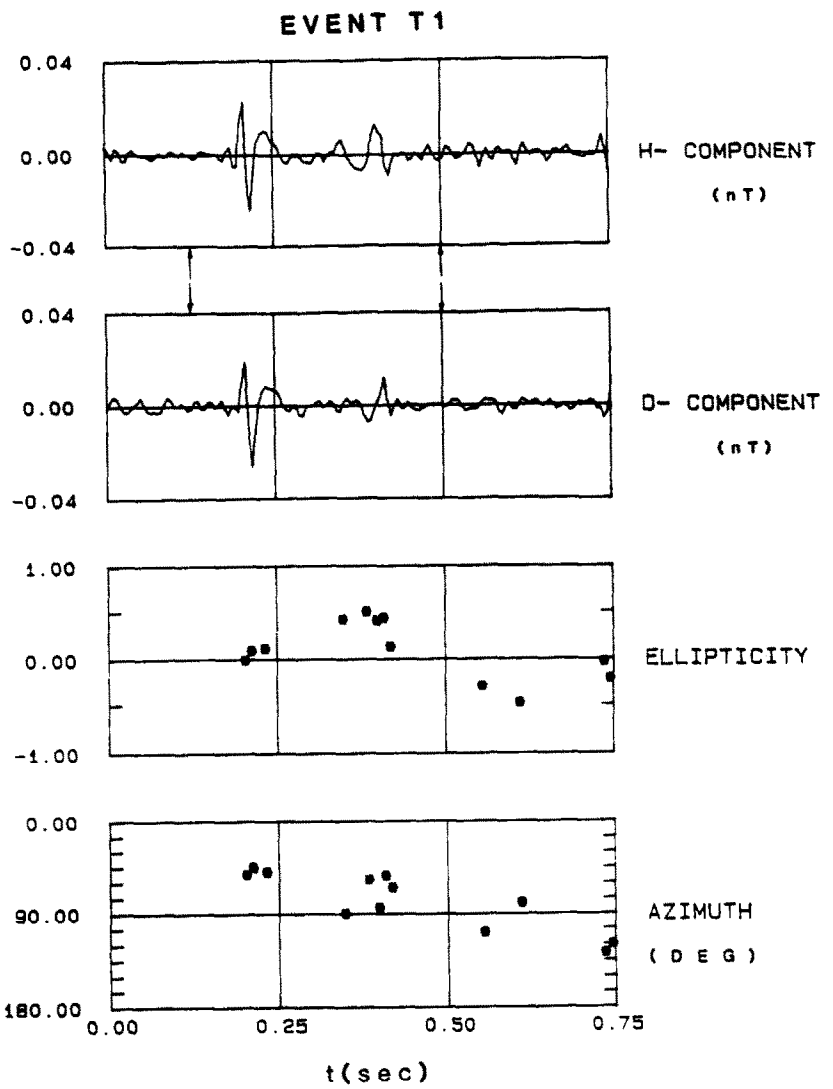

Fig. 4. Three examples of the time domain polarization analysis of impulsive transients. *H* and *D* correspond to the N–S and E–W magnetic components; real time separation of events T1–T2, 90.75 s, events T2–T3, 63.75 s. (*Continued over.*)

spectra of the impulsive sferics, annotated T1, T2 and T3. The spectra have been evaluated from the complex signal using the Maximum Entropy (ME) method (BURG, 1975). The high resolution capability of ME spectra for short data lengths permits the analysis of individual waveforms without interference from other sources. Thus only segments of the available data have been analysed. The segments are indicated in Figs. 3 and 4 with thin arrows.

It is immediately apparent that the spectral signatures of the three background events of Fig. 3 are very different. Recall that the example waveforms all possess different azimuths; in particular, events B1 and B3 are almost orthogonal. Our results indicate a variation of the spectral signature with azimuth. The same observation can be made for the impulsive transient events T1, T2 and T3. As indicated previously, the shape and trend of the spectral curves can be used to estimate the source–receiver separation. Care must be exercised while making such interpretations using the background field, as the theoretical results of JONES and KEMP (1970, 1971) refer to the excitation of the cavity by extra-large single discharges. In addition, the work assumes relatively simple source spectra. The spectra of the background and transient events (more representative of the above

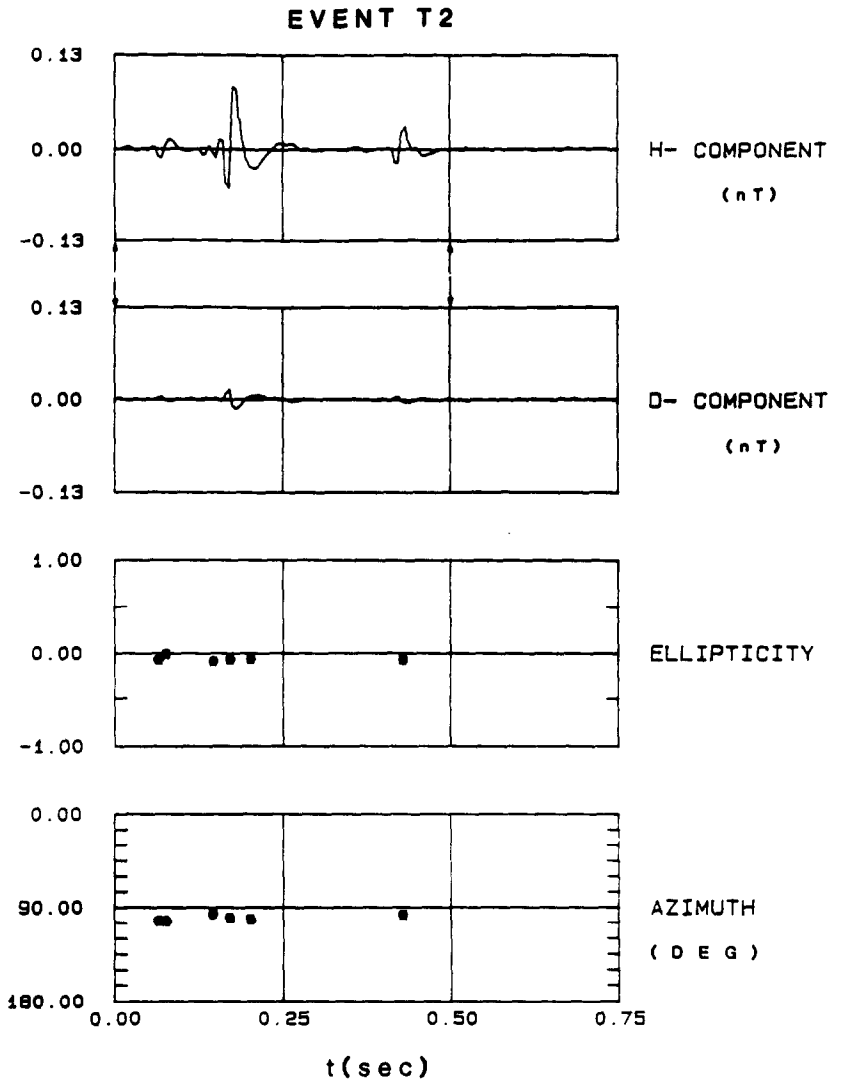

Fig. 4 continued. *(Continued over.)*

authors' models) display qualitative differences. The former possess sharper peaks and larger peak-to-trough ratios, possibly, because of the more severe attenuation experienced by weak sources in the cavity. However, events B2 and B3 display simple waveforms and do not appear to be the result of multiple sources. It must also be noted that our instrumentation, primarily intended for crustal sounding, includes a notch filter that was centred on 47.5 Hz. The notch was operational when the background events were collected. Frequencies above 40 Hz are therefore attenuated for spectra B1, B2 and B3.

With every caution we assert that the spectrum of event B2 is very similar in shape to the theoretical results of JONES and KEMP (1970, fig. 7) for a range (D) of 10,500 km. Event B3 possesses a spectrum which indicates a source less than 8000 km away. With regard to the impulsive transients, it can be inferred with confidence that event T2 represents a distant soruce ($D > 10{,}000$ km), whereas event T3 may represent a range (D) of less than 7000 km. The results presented above have been found to be repeatable. Waveforms selected on the basis of common azimuths display similar shapes and spectral signatures. We observe an association of spectral variability with azimuth and widely separated sources. We interpret

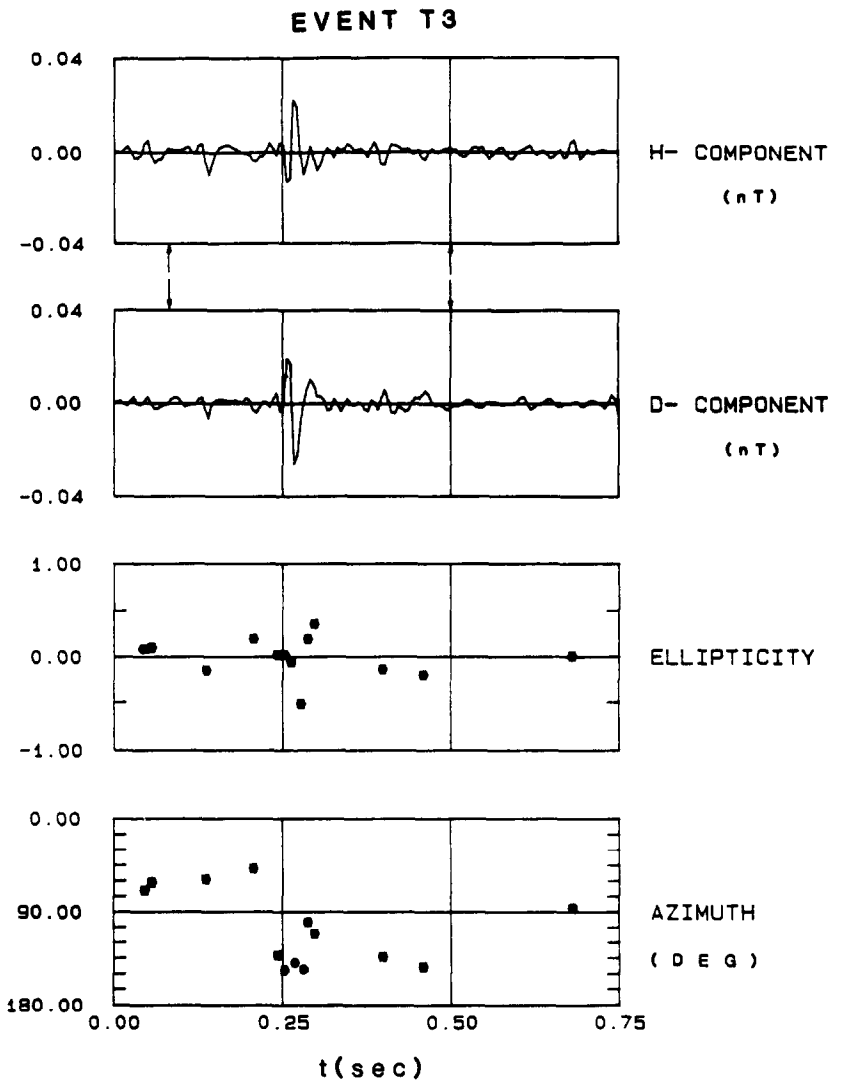

Fig. 4 continued.

this as being due to signals being received from different source locations and travelling over different paths.

It should be noted that the data used in the present study are not ideally suited to the determination of source locations. Such determinations are better made using spectra of the wave impedance, requiring measurements of the vertical electric field (KEMP, 1971; BLIOKH *et al.*, 1980). Our main conclusions arise from the results obtained from our time domain study of the polarization properties of the waveforms. The results show that many of the waveforms exhibit a stable linear polarization over several cycles. This behaviour can be interpreted as the direct arrival of a short path signal from a given source location. Such properties are most clearly exhibited by the larger transient events, but are also observed at the background level. We conclude that thunderstorm activity giving rise to sources which excite the Earth–ionosphere cavity can be simultaneous and therefore incoherent, but the effects from single sources are detectable even at the background level.

Acknowledgement—This paper is published with the approval of the Director, British Geological Survey (NERC).

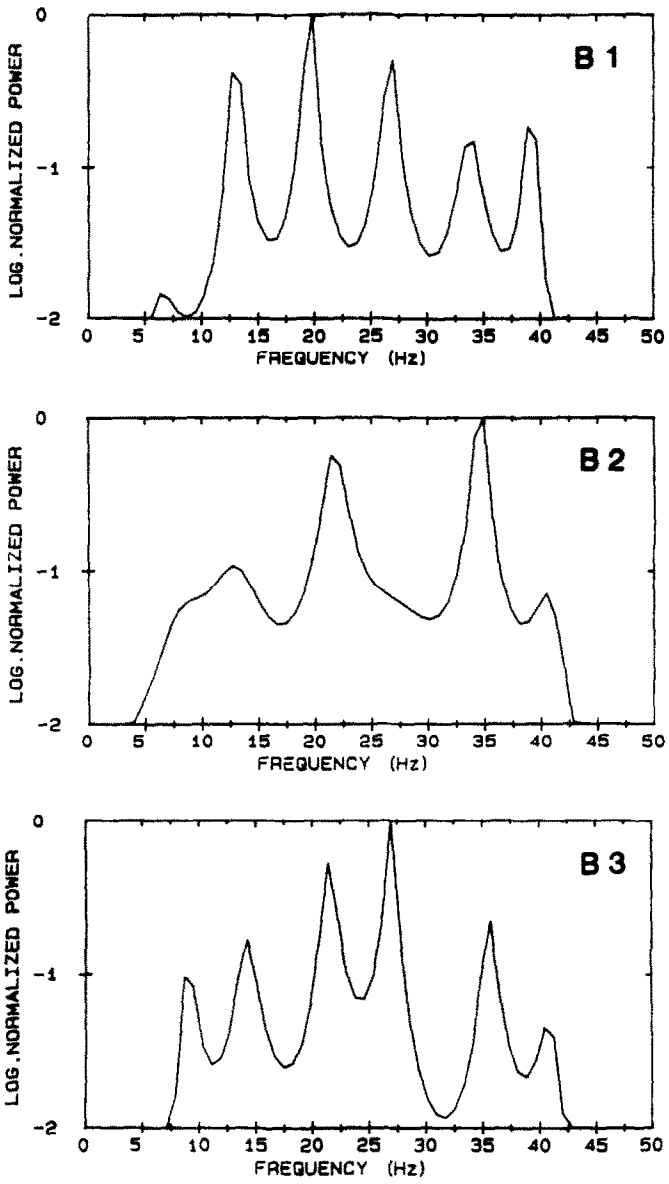

Fig. 5. The spectral signatures of the example sferics. Maximum Entropy power spectra of the azimuthal magnetic field. Data lengths analysed: event B1, 52 points (0.26 s); event B2, 48 points (0.24 s); event B3, 52 points (0.26 s) [filter length $M = 20$ used throughout]; event T1, 76 points (0.38 s); event T2, 100 points (0.50 s); event T3, 85 points (0.425 s) [filter length $M = 30$ used throughout]. (*Continued over.*)

REFERENCES

BEAMISH D. and TZANIS A. 1986 *J. atmos. terr. Phys.* **48**, 187.

BLIOKH H., NIKOLAENKO A. P. and FILIPPOV YU. F. 1980 *Schumann Resonances in the Earth–Ionosphere Cavity* (LLANWYN-JONES D., Ed.), IEE Electromagnetic Wave Series 9. P. Peregrinus Ltd, Stevenage.

BORN M. and WOLF E. 1959 *Principles of Optics*. Pergamon Press, New York.

BURG J. P. 1975 Ph.D. Thesis, Stanford University, Stanford, California.

FOWLER R. A., KOTICK B. J. and ELLIOTT R. D. 1967 *J. geophys. Res.* **72**, 2872.

GABOR D. 1946 *J. Instn elect. Engrs* **93**, 429.

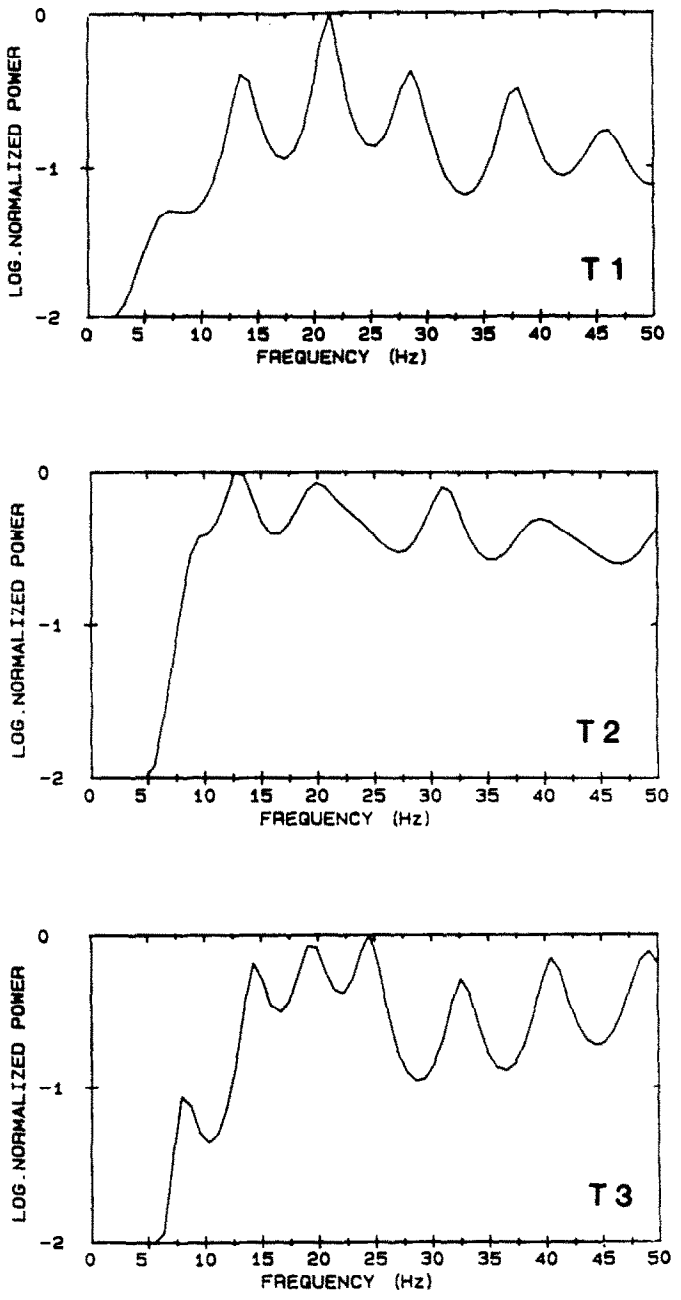

Fig. 5 continued.

Jones D. L. and Kemp D. T.	1970	*J. atmos. terr. Phys.* **32**, 1095.
Jones D. L. and Kemp D. T.	1971	*J. atmos. terr. Phys.* **33**, 557.
Kemp D. T.	1971	*J. atmos. terr. Phys.* **33**, 919.
Kodera K., Gendrin R. and De Villedary C.	1977	*J. geophys. Res.* **82**, 1245.
Madden T. and Thomson W.	1965	*Rev. Geophys.* **3**, 211.
Turman B. N. and Edgar B. C.	1982	*J. geophys. Res.* **87**, 1191.
Tzanis A. and Beamish D.	1986	Geomagnetism Research Group, Internal Report 86/13, British Geological Survey.